

Supporting Information

Rohr et al. 10.1073/pnas.1415971112

SI Background

Trematode Life Cycle. In our focal trematode–amphibian system, adult trematodes are found in vertebrate definitive hosts, where they reproduce sexually. Trematode eggs are released into waterbodies in the excrement of the definitive host. Miracidia hatch from the eggs and infect snails, the first intermediate host. These miracidia develop into sporocysts. Through asexual reproduction, the sporocysts produce, and the snail sheds free-living trematode cercariae. The cercariae, in turn, swim through the water searching for tadpoles, the second intermediate host. Two of the three focal cercariae in our experiment use proteolytic enzymes to encyst as metacercariae s.c. The last trematode, *Echinostoma trivolvis*, crawls up the amphibian cloaca and encysts as metacercariae in the kidneys. Finally, if an infected tadpole is consumed by a suitable definitive host, the life cycle is completed (1).

Taxa That Consume Cercariae. Several taxa are known to consume several species of free-living cercariae. Many of the seminal studies were conducted on *Schistosoma mansoni* cercariae, a parasite that infects humans. Rowan (2) and Knight et al. (3) reported that the guppy *Lebistes reticulatus* consume *S. mansoni* cercariae. Christensen (4) found that *Daphnia pulex* and *Daphnia longispina* (Cladocera), *Notodromas monacha* and *Cypria ophthalmica* (Ostracoda), and *L. reticulatus* were predators of *S. mansoni* cercariae. Additionally, experiments conducted by Christensen (4) and Christensen et al. (5) showed that predation of cercariae reduced transmission of *S. mansoni* to laboratory mice.

Kaplan et al. (6) presented six species of native estuarine fishes with 10 native trematode species. Many of the fishes engorged on cercariae. Moreover, they found evidence that fish also consumed cercariae under field conditions.

Schotthoefer et al. (7) showed that *Hydra* spp., damselfly (Odonata, Coenagrionidae) larvae, dragonfly (Odonata, Libellulidae) larvae, and copepods (Cyclopoida) consumed *Ribeiroia ondatrae* cercariae. Damselfly and dragonfly larvae were particularly voracious, in some cases consuming 80–90% of the cercariae offered within 10 min. In most cases, the foraging rates of predators on cercariae were not significantly affected by alternative prey.

Orlofske et al. (8) revealed that California newt larvae (*Taricha torosa*), western mosquitofish (*Gambusia affinis*), damselfly larvae (*Enallagma* spp. or *Lestes* spp.), and California clam shrimp (*Cyzicus californicus*) all depredated *R. ondatrae* cercariae. Moreover, in laboratory experiments, newt larvae and damselfly larvae reduced transmission of cercariae to tadpole hosts. Bioassays indicated that these predators consumed cercariae even in the presence of alternative prey.

SI Materials and Methods

Wetland Survey.

Overview. To quantify the diversity of amphibians and macroinvertebrates we conducted daytime visual time- and area-constrained dip-net sampling, adjusting effort according to the size of the wetland. Vegetation was quantified by randomly placing three 10-m transects within each community type around each wetland, and the line-intercept method was used to record relative cover of each plant species under or over the line. Macroinvertebrate and vegetation sampling occurred during three visits (March–April, May–June, and July–August). Snails were identified to species and arthropods were identified to family or below. We wanted to avoid destructively sampling macroinvertebrates and thus obtained presence–absence information for

each snail and arthropod captured and abundance information for the dominant snail species, *P. trivolvis*.

On two visits (one in April–May and a second in June–July) we obtained water samples and attempted to collect a minimum of 15 recently metamorphosed *Rana pipiens* for parasite assessments and 25 for pathology studies including immune cell quantification. We quantified nitrate, phosphate, calcium (necessary for shell production), and atrazine (herbicide) levels from the water samples because each can promote snail population growth (9, 10). Amphibians were necropsied and their macroparasites were identified and quantified. Additionally, we quantified melanomacrophages from the hematoxylin and eosin-stained and sectioned livers of the amphibians because they are important immune cells for fighting trematodes (10).

Wetland selection and biotic sampling. Candidate wetlands were identified on National Wetland Inventory maps and selected for inclusion in the study following field reconnaissance within the Broadleaf Forest Ecoregion in Minnesota. Final criteria for inclusion in the analyses were (i) classification as a palustrine aquatic bed or emergent wetland, (ii) 0.5–5.0 ha in size, (iii) degree of landscape disturbance perceived by field assessments, (iv) landowner permission, (v) the presence of *R. pipiens*, and (vi) intermediate host (snail) abundance. Attempts were also made to include only wetlands that were at least 2 km apart to reduce spatial autocorrelation.

Analyte sampling and quantification. Water samples were taken just below the surface in the deepest area of the wetlands using a pole sampler (Nasco Swing Sampler 3228) and an amber glass collecting bottle, with care to avoid surface plants and other floating matter. Water was then decanted into a series of dedicated bottles specifically prepared for groups of analytes, including base neutral organics, acid herbicides, paraquat/diquat, metals, glyphosate, carbamate insecticides, and inorganic ions. Water for metals analysis was stabilized with ultra-grade nitric acid. Water for diquat and paraquat assays was stabilized with reagent-grade sulfuric acid. Finally, water for carbamate analysis was stabilized with monochloroacetic acid buffer. The samples were immediately chilled on ice and transferred on cold packs to the laboratory every 2 to 3 d.

Seven sediment cores were collected from each wetland in 0.6 m of water at approximately equidistant points around the wetland edge using a soil sampler auger (AMS basic soil sampler 3106) fitted with a 25- × 5-cm acrylic plastic sleeve. Samples were immediately placed and remained on ice to maintain 4 °C. Samples were sent to the analytical laboratory within 3 d of collection. The coring technique allowed us to collect sediment from the sediment–water interface, which is most likely to be actively engaged in exchange with the overlying water and in contact with amphibians. For three of the seven cores, the top 15 cm of each core was sent to the South Dakota State University Soil Analysis Laboratory for determination of organic matter content, phosphorus, and texture. Loss-on-ignition was used to measure organic matter content. Extractable P was determined using the sodium method. The remaining four cores were sent to the Illinois Waste Management and Research Center (recently renamed the Illinois Sustainable Technology Center) at the University of Illinois for quantification of elements and organic contaminants.

The following standard US EPA methods were used to quantify analytes with occasional minor modifications: 200.8 for metals and elements in tissue; 1631 for mercury in digested samples; 525.2 for base neutral organic compounds in water; 3545, 3630C, and 3640A for base neutral organic compounds in sediment and tissue; 8151A, 515.1, and 515.2 for acid herbicide compounds in water and sediment; 547 for glyphosate in water; 549.1, Revision

1.0 for paraquat and diquat in water; and 531.1, Revision 3.0 for N-methylcarbamoyloxamines and N-methylcarbamates in water. **Quality assurance in analyte quantifications.** Duplicate or triplicate water samples were collected in several ponds during each sampling survey at the same location as the pond samples. An additional “mix” sample was taken, well away from the usual collection site, in selected ponds to test the assumption that the water of the ponds was well mixed. Trip blank water samples were carried to the field, stored with the samples, and delivered with the samples to the laboratory.

During the analytical process, several types of quality assurance samples/analyses were used, including analytical and matrix spikes, analytical replicates, and laboratory blanks. Instruments were calibrated according to manufacturer and/or method guidelines. Calibration curves were prepared from the reporting limit through most of the linear range of the instruments. Samples yielding results greater than the highest standard were diluted and rerun. Calibration check standards were run for most of the analyses. Internal standards were used in all GC/MS and ICP/MS analyses. Surrogate organic compounds were added to GC/MS samples before extraction and were monitored for recovery as an overall measure of the performance and consistency of the entire analytical procedure. Recoveries typically were above 90%.

Frog collection, pathology, and parasitology. Frogs were delivered within three days of collection to either the National Wildlife Health Center for parasitology evaluations or the University of Illinois, College of Veterinary Medicine for pathology assessments. Collections occurred in July and August of 1999. Pathology and parasitology examinations occurred after frogs were killed and followed standard protocols. Melanomacrophage aggregates were identified on hematoxylin and eosin-stained sections with a light microscope. Encysted metacercariae in the musculature were identified and enumerated by examining the cleared and stained specimens under a dissecting microscope (Fig. S2). Fixed parasite specimens were prepared for identification following standard protocols. Voucher specimens of parasites were deposited in the USDA National Parasite Collections, Beltsville, Maryland and cleared and stained frogs were deposited in the Bell Museum of Natural History, University of Minnesota, Minneapolis-St. Paul, Minnesota (collection numbers 14624–15168).

Odonate Foraging Experiment. For each trial, we used a pipette and a dissecting microscope to collect 50 cercariae from a mixture of seven infected *Planorbella trivolvis* snails. Cercariae were transferred to a plastic predation arena (8.5 × 6.5 × 2.3 cm) containing 100 mL of double-filtered (through 75- μ m Nitex to remove any cercariae, which measure >200 μ m) pond water and an odonate larva. After 1 h, we counted the number of cercariae that remained. The number of replicates per odonate species ranged from 11 to 28 depending on their availability. Odonates and snails were collected from ponds in Boyce and Hume, Virginia and were maintained on a 14:10 light-dark cycle. Odonates were not fed the day before the trials. In the first foraging experiment, we used *E. trivolvis* cercariae. In the second foraging experiment, we used a Plagiorchid cercariae.

Mesocosm Experiment. This experiment was conducted in clear rectangular plastic tubs (38 × 25 × 15 cm filled with 10 L of filtered pond water) with 6 10-cm pieces of black nylon rope attached to the bottom of each tub in a uniform distribution to provide perches for the larval odonates. Each tub had 10 *R. clamitans* tadpoles (Gosner stage 25; hatched from two egg masses ordered from Charles D. Sullivan Co. Inc.), a single *P. trivolvis* snail rotated among tubs, and food for the tadpoles and snails (1 g of coarsely ground rabbit food and a 1- × 1-cm portion of frozen spinach). The experiment was conducted at the University of Virginia’s Blandy Experimental Farm, on a 14:10 light-dark cycle, and included a total of 64 experimental units.

SI Results and Discussion

Mesocosm Experiment. We hypothesized that odonate exposure might reduce foraging activity and thus the resources available for immunological resistance to cercariae that could account for the observed infection patterns across treatments. We assumed that any significant reduction in tadpole body mass per individual would reflect a reduction in overall resources that could be dedicated toward immunity. We found no evidence of any differences in tadpole body mass as a function of odonate density, diversity, or their interaction ($F_{1,53} < 0.321$, $P > 0.573$) or the densities of any specific odonate species or interactions between species ($F_{1,49} < 2.467$, $P > 0.122$). Although we cannot discount a reduction in relative investment in immunity, or, in other words, a redistribution of resources from immunity to antipredator defenses, our data provide little evidence that any of the treatments reduced the absolute level of resources for immunological defenses against cercariae.

We then examined the results of our second cercarial foraging experiment to assess whether interactions among odonate species affected cercarial foraging and thus infections in tadpoles. Tripling odonate density did not triple the overall foraging rate within a species (Fig. S3), suggesting that the relationship between odonate density and cercarial foraging is nonlinear and odonate interactions, regardless of species, can reduce cercarial foraging rates (11). Nevertheless, cercarial foraging rates were generally independent of interspecific interactions among odonates (Fig. S3), consistent with the lack of interactions among odonate species on metacercarial infections per tadpole and suggesting that odonate interspecific interactions were not capable of explaining the observed pattern in metacercarial infections per tadpole as a function of diversity.

Increasing odonate diversity from two to three species at the high odonate density caused an increase in metacercarial infections and a concomitant drop in tadpole activity that was surprisingly inconsistent with the number of *I. verticalis* in this treatment (Fig. 2A and C). For whatever reason, tadpoles seemed to perceive this treatment as the most dangerous (apart from 12 *I. verticalis*) as reflected by their activity (Figs. 2C and 4B and C). Nevertheless, such a high density of odonates seems unlikely to be common in the field (12).

Although we did not encounter any wetlands in our field survey without odonates, indicating that this treatment is also of rare ecological relevance, we would be remiss if we did not briefly discuss the lower-than-expected metacercarial infections in this treatment. Metacercarial loads likely increased from zero to one odonate species at low odonate densities because the reduction in cercarial exposure associated with the cercarial foraging was not as great as the increase in cercarial rates of contact with tadpoles caused by the decrease in tadpole activity (Fig. 2C). At the high density, we suspect that monospecific odonate treatments provided a sufficient amount of cercarial foraging to offset the effects of reduced anticercarial behaviors of tadpoles associated with this treatment relative to controls (Fig. 2A and C).

Mathematical Model. Here we reiterate and further explain the mathematical model that we used to capture long-term dynamics and feedbacks that are important to IGP. The model tracks changes in the densities of focal (could be second intermediate or definitive) hosts, H , parasites that successfully infected hosts, P , intermediate hosts, I , and free-living parasites, Z using differential equations (Eqs. 1a–1d):

$$\frac{dH}{dt} = b_H \left(1 - \frac{H}{K_H} \right) H - d_H H - f_H C H - \nu P \quad [1a]$$

$$\frac{dP}{dt} = \varepsilon \sigma H Z - (d_H + f_H C + \mu + \nu) P - \nu \frac{P^2(\theta + 1)}{H\theta} \quad [1b]$$

$$\frac{dI}{dt} = b_I \left(1 - \frac{I}{K_I}\right) I - d_I I - f_I C I \quad [1c]$$

$$\frac{dZ}{dt} = \gamma \left(\frac{P}{P+q}\right) I - \varepsilon H Z - f_Z C Z - d_Z Z. \quad [1d]$$

Focal hosts increase through density-dependent births, as determined by a maximum rate, b_H , and a host carrying capacity, K_H (Eq. 1a). Focal hosts are lost because of background deaths, at mortality rate, d_H , predation by consumers, C , at per capita feeding rate, f_H , and from parasitic infection, with virulence on survival, v . Parasitic infections of focal hosts, P , increase when hosts become infected by free-living parasites, Z . Following exposure (at per capita exposure rate, ε), hosts can become infected according to their per-parasite susceptibility, σ ($0 \leq \sigma \leq 1$; Eq. 1b). Parasitic infections decrease when hosts die (from background mortality, predation by consumers, or parasite virulence). The final term in Eq. 1b accounts for additional losses from parasite-induced mortality that occur because parasites are aggregated in focal hosts, indexed by θ , the aggregation parameter of the negative binomial distribution. Intermediate hosts also increase through density-dependent births, as determined by a maximum rate, b_I , and their carrying capacity, K_I (Eq. 1c). They are also lost from background deaths, at mortality rate, d_I , and predation by consumers, C , at per capita feeding rate, f_I . Finally, free-living parasites increase because of release (at per capita rate γ) by infected intermediate hosts (with infections assumed to be a saturating function of P , governed by the half-saturation constant, q ; Eq. 1d). Free-living parasites are then lost following contact with focal hosts, ε , predation by consumers, f_Z , or from background mortality, d_Z .

The model assumes that the intermediate host population produces free-living parasites at a constant per capita rate. Additionally, we chose not to dynamically couple the predator guild to host or free-living parasite densities because most, if not all, of the predators in our focal system are broad generalists. Although a full analytical solution for this model is intractable, we can simplify the model somewhat. The dynamics of the intermediate host population, I , do not depend on any of the other state variables in the system. Therefore, we can solve for the equilibrium density of intermediate hosts, I^* , place this term in the equation for free-living parasites (dZ/dt , Eq. 1d), and reduce the system from four dimensions to three:

$$\frac{dH}{dt} = b_H \left(1 - \frac{H}{K_H}\right) H - d_H H - f_H C H - v P \quad [2a]$$

$$\frac{dP}{dt} = \varepsilon \sigma H Z - (d_H + f_H C + \mu + v) P - v \frac{P^2(\theta + 1)}{H\theta} \quad [2b]$$

$$\frac{dZ}{dt} = \gamma \left(\frac{P}{P+q}\right) I^* - \varepsilon H Z - f_Z C Z - d_Z Z. \quad [2c]$$

Solving for I^* from Eq. 1c yields

$$I^* = \left(\frac{b_I - (d_I + f_I C)}{b_I}\right) K_I, \quad [3]$$

which is the carrying capacity of intermediate hosts tempered by the relative population growth rate of intermediate hosts (numerator: birth rate minus total loss rate) divided by the birth rate of intermediate hosts.

Although the model remains intractable, we gained insight by examining two partial solutions for mean parasite burden at

equilibrium, P^*/H^* and Z^* , by setting Eqs. 1a and 1b equal to zero, respectively. We also numerically simulated the model across a range of reasonable values for the predation rate on hosts, f_H , and free-living parasites, f_Z , with the Isoda function from the deSolve package in R statistical software and determined the equilibrium values of (i) focal host density, (ii) parasite density, (iii) free-living parasite density, and (iv) mean parasite burden in focal hosts for each simulation. See Fig. 5 and Fig. S4 for the state variables and parameters used in the epidemiological model.

Consumption of free-living parasites increases equilibrium densities of focal hosts and reduces the total number and mean burden of parasites among focal hosts, as well as the density of free-living parasites (Fig. S4 A–D). The consequences of predation on parasites can be illustrated by calculating the proportion of free-living parasites that contact focal hosts before dying, $P(\text{Contact any focal host})$. This quantity is determined, by definition, as the ratio of the overall contact rate with focal hosts and the total loss rate of free-living parasites. All else equal, the proportion of parasites that successfully contact focal hosts decreases monotonically with predation on parasites, f_Z :

$$P(\text{Contact any focal host}) = \frac{\varepsilon H}{\varepsilon H + d_Z + f_Z C}. \quad [S1]$$

Predation on focal hosts directly reduces equilibrium focal host density (Fig. S4E). It also reduces the total density of parasites (Fig. S4F). This occurs for two reasons. First, consumption of focal hosts destroys parasites that had successfully infected those hosts. Second, the reduction in focal host density reduces the probability that a free-living parasite will successfully contact a focal host before death (because this probability is a monotonically increasing function of focal host density, Eq. S1). Initially, predation on focal hosts reduces the equilibrium mean burden. However, as predation on focal hosts increases, the equilibrium density of free-living parasites and the mean burden increases as well (Fig. S4 G and H). This unimodal response can even lead to equilibrium mean burdens that exceed the predation-free case.

Why do mean burdens increase with predation on focal hosts even when the total density of parasites within focal hosts decreases? Again, the answer is related to rates of contact among focal hosts and free-living parasites. Eq. S1 represents the probability that a free-living parasite contacts any focal host before dying. However, mean parasite burden is more directly related to the per-host contact rate (i.e., the probability that a parasite contacts a particular focal host before dying). This per-host contact rate, $P(\text{Contact a given focal host})$, is the total contact rate (Eq. S2) divided by focal host density:

$$P(\text{Contact a given focal host}) = \frac{\varepsilon}{\varepsilon H + d_Z + f_Z C}. \quad [S2]$$

This is analogous to the fact that per capita mortality rates of prey equal the predator's functional response divided by prey density (13). This per capita contact rate (Eq. S2) is now a monotonically decreasing function of focal host density. This occurs specifically because exposure of hosts depletes free-living parasites from the environment (i.e., no one parasite can invade or infect two hosts). Therefore, as predators reduce the total density of focal hosts from the environment, the per capita risk of exposure (and therefore infection) can actually increase for focal hosts that remain. This result is supported by a partial analytical solution for equilibrium mean parasite burden, P^*/H^* , derived from Eq. 1a:

$$\frac{P^*}{H^*} = \frac{b_H \left(1 - \frac{H^*}{K_H}\right) - d_H - f_H C}{v}. \quad [S3]$$

Predation on hosts, $f_H C$ (the third term in the numerator of Eq. S3), directly reduces mean burden. However, predation can also depress equilibrium host density, H^* , increasing the density dependent birth rate of hosts (the first term in the numerator of Eq. S3). If the increase in density-dependent birth rate outweighs the direct effect of predation, then predation on hosts increases mean burdens. Thus, predators can increase mean burdens by causing greater relative decreases in host density than parasite density (Fig. 5 and Fig. S4 E–H).

In our model, density dependence in the focal host population facilitates this pattern. Here we chose to represent density dependence among hosts with logistic population growth. However, intraspecific density dependence can be nonlinear, and over some ranges of population density for some species it can act weakly. If density dependence only weakly affects the focal host population, then IGP-driven increases in parasitism might not occur as strongly. Thus, the specific details regarding density dependence may influence the potential and magnitude of IGP-driven increases in parasitism across systems.

Another effect (involving the density of free-living parasites) arises in this model that contributes to increasing parasite burdens with predation. Predation on hosts causes a reduction in the total number of parasites in focal hosts (P^*) but simultaneously causes the density of free-living parasites in the environment (Z^*) to increase (Fig. S4 F and G). Again, we turn to a partial solution for Z^* using Eq. 1b. First, assuming H is positive, we divide both sides by H :

$$\frac{1}{H} \frac{dP}{dt} = \varepsilon \sigma Z - (d_H + f_H C + \mu + \nu) \frac{P}{H} - v \left(\frac{P}{H} \right)^2 \frac{(\theta + 1)}{\theta}. \quad [\text{S4}]$$

At equilibrium, the right-hand side of this equation is equal to zero:

$$0 = \varepsilon \sigma Z^* - (d_H + f_H C + \mu + \nu) \frac{P^*}{H^*} - v \left(\frac{P^*}{H^*} \right)^2 \frac{(\theta + 1)}{\theta}. \quad [\text{S5}]$$

Rearranging this equation for Z^* yields this partial solution:

$$Z^* = \left((d_H + f_H C + \mu + \nu) \frac{P^*}{H^*} + v \left(\frac{P^*}{H^*} \right)^2 \frac{(\theta + 1)}{\theta} \right) / (\varepsilon \sigma). \quad [\text{S6}]$$

Here Z^* is an increasing function of both predation on hosts ($f_H C$) and mean equilibrium burden (P^*/H^*). If we assume that Z^* is constant, then as $f_H C$ increases, P^*/H^* would have to decrease. However, this does not occur; P^*/H^* increases, and therefore Z^* also increases with predation on hosts (Fig. S4G). This occurs because hosts deplete free-living parasites during the transmission process. If there are fewer hosts, then there is less depletion via transmission. This decreases the total loss rate of free-living parasites from the environment (denominator of Eq. S1), and therefore increases the density of free-living parasites. Thus, despite a lower total density of parasites in focal hosts, predators can cause an increase in the density of free-living parasites in the environment (Fig. 5 and Fig. S4 E–H). This provides a testable prediction of this model: Predators that disproportionately attack hosts could simultaneously boost mean parasite burden and the density of free-living parasites.

Some predator species can consume free-living parasites and focal hosts (i.e., IG predators). Therefore, we simulated our model across a 2D gradient of predation rates on parasites and focal hosts. As in the simpler cases above, predators that only consumed free-living parasites reduced disease efficiently. In fact,

for all rates of predation on focal hosts, increasing the predation rate on parasites resulted in higher focal host density, reduced the population of parasites infecting focal hosts, and reduced mean burdens (Fig. 5). Increasing predation on focal hosts always reduced the total number of parasites successfully infecting focal hosts (Fig. 5B). In contrast, increasing predation rates on hosts had a nonlinear effect on equilibrium mean parasite burden (Fig. 5C), even though increasing predation on hosts always reduced host density (Fig. 5A). This recaptured the pattern from the previous simulation (Fig. S4 E–H). Initially, increases in predation on focal hosts reduce mean burden, but further increases in predation minimally reduce mean burdens. High rates of predation on focal hosts can elevate equilibrium mean burdens substantially, especially if predation on free-living parasites is low (Fig. 5C, lower right).

Similarities Between Predator Diversity–Biocontrol Literature and Results of This Study.

Our findings have many similarities with the generalities that have emerged from the predator diversity–biocontrol literature, suggesting that our work might inform both disease management and pest control. First, similar to evidence that guilds of predators on average control pests better than single predator species (14–16), our findings suggest that entire guilds of predators can also regulate infections in hosts. Thus, managing predator assemblages might be more effective than managing single predator species to control disease. As an example, schistosomiasis is a debilitating trematode disease of humans in the tropics and management efforts have focused on introducing single fish or crustacean predator species to control this disease (17, 18). Our results suggest that research should compare the value of management that maximizes the abundance and/or diversity of snail and cercarial predators to that of current approaches focused on single predator species.

Second, and again similar to our results, the predator diversity–biocontrol literature provides evidence that IG predation and nonconsumptive effects influence the strength of biocontrol offered by predator diversity (14–16, 19). In our model, the strength of predator control of parasites was not considerably different if the predator consumed the parasite directly or coincidentally by consuming infected snails. Likewise, in a meta-analysis, biocontrol of herbivore pests was not reduced when IG predators consumed parasitized herbivores, thereby consuming both the herbivore and developing parasitoid (20). Our model also revealed that IG predators that strongly prefer free-living parasites over hosts suppress parasite densities, whereas IG predators that strongly prefer hosts over free-living parasites could increase parasite densities per host by increasing the per capita exposure rate of the surviving hosts. Similarly, and consistent with IG predation theory (21), a meta-analysis revealed that the addition of non-IG predators generally suppressed pest prey populations, but IG predators, especially those that consumed one another, could even increase pests (19).

These similarities between the effects of IG predators and predator diversity on the control of both pathogens and pests suggest that there may be general mechanisms for pest control regardless of whether the pest is a pathogen or consumer. Indeed, our results suggest that the general conclusion for disease control might match that for pest control. That is, releasing multiple non-IG predators will likely provide better pathogen suppression than releasing a single control agent (14), but the release of IG predators could decrease or increase pathogens and thus the release of the single best control agent might provide better suppression of pathogen populations on average than the release of IG predators (19). Regardless of whether this conclusion holds, it seems clear that biocontrol research might inform disease management, and vice versa (22).

Disclaimer. Although the research described herein has been funded by several granting agencies, this report has not been subjected to their review and therefore does not necessarily reflect their points of view. Accordingly, no official endorsement should be inferred.

1. Koprivnikar J, et al. (2012) Macroparasite infections of amphibians: What can they tell us? *EcoHealth* 9(3):342–360.
2. Rowan WB (1958) Daily periodicity of *Schistosoma mansoni* cercariae in Puerto Rican waters. *Am J Trop Med Hyg* 7(4):374–381.
3. Knight WB, Ritchie LS, Liard F, Chiribog J (1970) Cercariophagic activity of guppy fish (*Lebistes reticulatus*) detected by cercariae labeled with radiosenium (75 SE). *Am J Trop Med Hyg* 19(4):620.
4. Christensen NO (1979) *Schistosoma mansoni*: Interference with cercarial host-finding by various aquatic organisms. *J Helminthol* 53(1):7–14.
5. Christensen NO, Frandsen F, Nansen P (1980) The interaction of some environmental factors influencing *Schistosoma mansoni* cercarial host-finding. *J Helminthol* 54(3): 203–205.
6. Kaplan AT, Rebhal S, Lafferty KD, Kuris AM (2009) Small estuarine fishes feed on large trematode cercariae: Lab and field investigations. *J Parasitol* 95(2):477–480.
7. Schotthoefer AM, Labak KM, Beasley VR (2007) *Ribeiroia ondatrae* cercariae are consumed by aquatic invertebrate predators. *J Parasitol* 93(5):1240–1243.
8. Orlofske SA, Jadin RC, Hoverman JT, Johnson PTJ (2014) Predation and disease: Understanding the effects of predators at several trophic levels on pathogen transmission. *Freshw Biol* 59(5):1064–1075.
9. Johnson PTJ, et al. (2007) Aquatic eutrophication promotes pathogenic infection in amphibians. *Proc Natl Acad Sci USA* 104(40):15781–15786.
10. Rohr JR, et al. (2008) Agrochemicals increase trematode infections in a declining amphibian species. *Nature* 455(7217):1235–1239.
11. Civitello DJ, Pearsall S, Duffy MA, Hall SR (2013) Parasite consumption and host interference can inhibit disease spread in dense populations. *Ecol Lett* 16(5):626–634.
12. Corbett PS (1999) *Dragonflies: Ecology and Behavior of Odonata* (Cornell Univ Press, Ithaca, NY).
13. Sarnelle O, Wilson AE (2008) Type III functional response in *Daphnia*. *Ecology* 89(6): 1723–1732.
14. Griffin JN, Byrnes JEK, Cardinale BJ (2013) Effects of predator richness on prey suppression: A meta-analysis. *Ecology* 94(10):2180–2187.
15. Bruno JF, Cardinale BJ (2008) Cascading effects of predator richness. *Front Ecol Environ* 6(10):539–546.
16. Finke DL, Snyder WE (2010) Conserving the benefits of predator biodiversity. *Biol Conserv* 143(10):2260–2269.
17. Mkoji GM, et al. (1999) Impact of the crayfish *Procambarus clarkii* on *Schistosoma haematobium* transmission in Kenya. *Am J Trop Med Hyg* 61(5):751–759.
18. Chimbari MJ, Madsen H, Ndamba J (1997) Laboratory experiments on snail predation by *Sargochromis codringtoni*, a candidate for biological control of the snails that transmit schistosomiasis. *Ann Trop Med Parasitol* 91(1):95–102.
19. Vance-Chalcraft HD, Rosenheim JA, Vonesh JR, Osenberg CW, Sih A (2007) The influence of intraguild predation on prey suppression and prey release: A meta-analysis. *Ecology* 88(11):2689–2696.
20. Rosenheim JA, Harmon JP (2006) The influence of intraguild predation on the suppression of a shared prey population: an empirical assessment. *Trophic and Guild Interactions in Biological Control*, eds Brodeur J, Boivin G (Springer, Dordrecht, The Netherlands), pp 1–20.
21. Polis GA, Myers CA, Holt RD (1989) The ecology and evolution of intraguild predation: Potential competitors that eat each other. *Annu Rev Ecol Syst* 20:297–330.
22. Raffel TR, Martin LB, Rohr JR (2008) Parasites as predators: Unifying natural enemy ecology. *Trends Ecol Evol* 23(11):610–618.

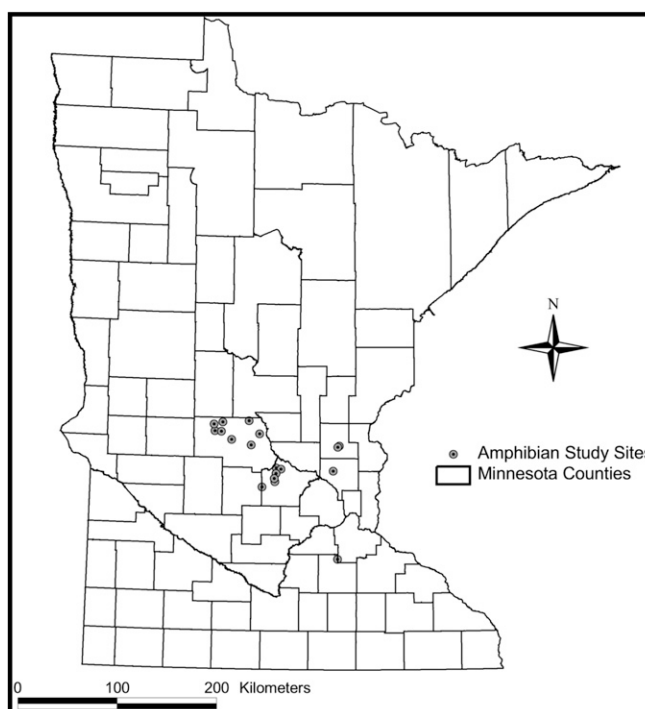


Fig. S1. Map of wetlands used in this study.

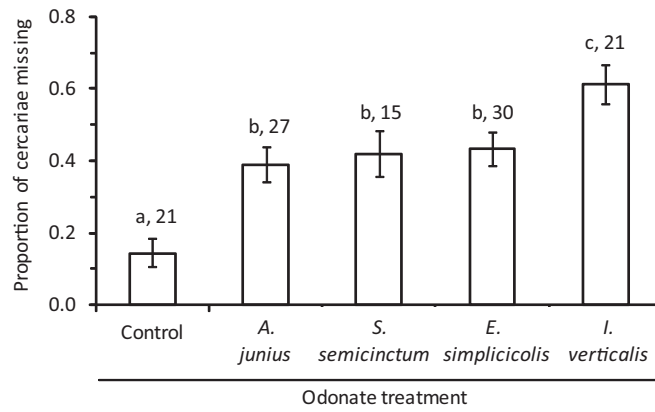


Fig. S2. Mean (\pm SE) predation rates of four species of odonate larvae (*Anax junius*, *Erythemis simplicicolis*, *Sympetrum semicinctorum*, *Ischnura verticalis*) on cercariae of *Echinostoma trivolvis* during 1-h trials. Bars with different letters are significantly different from one another ($P < 0.05$) and numbers above the bars indicate sample sizes.

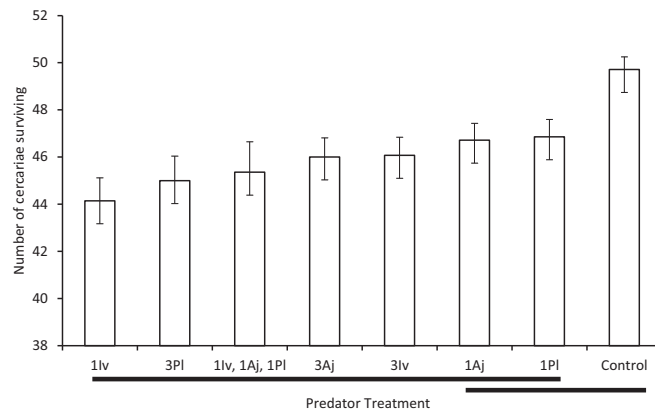


Fig. S3. Survival of cercariae in each treatment (lv = *Ischnura verticalis*, PI = *Pachydiplax longipennis*, Aj = *Anax junius*). Treatments connected by bars are not significantly different as determined by post hoc test. Shown are means \pm 1 SE.

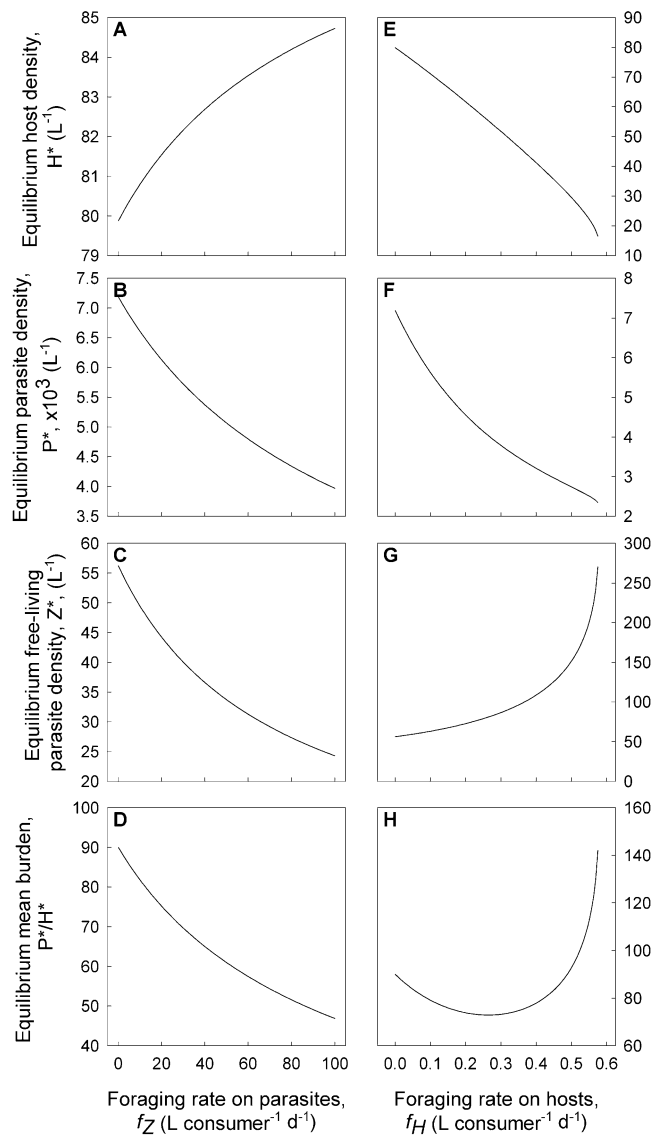


Fig. 54. Epidemiological consequences of predation on (A–D) free-living parasites and (E–H) focal hosts. Increasing predation on free-living parasites (A) increases the equilibrium density of focal hosts, (B) decreases the equilibrium density of parasitic infections in focal hosts, (C) decreases the density of free-living parasites, and (D) reduces the equilibrium mean burden of parasites within focal hosts. In contrast, predation on focal hosts decreases (E) equilibrium focal host density and (F) the equilibrium density of parasitic infections in focal hosts. However, predation on focal hosts can cause a substantial increase in the (G) density of free-living parasites and (H) mean parasite burden for focal hosts at equilibrium (especially at high predation rates). No predation on focal hosts in A–D or on parasites in E–H. All other simulation parameters: $b_H = 1$, $K_H = 100$, $d_H = 1$, $C = 1$, $v = 0.001125$, $\varepsilon = 1$, $\sigma = 1$, $\mu = 0.1$, $\theta = 10$, $b_I = 1$, $K_I = 100$, $d_I = 0.1$, $\gamma = 50$, $q = 10$, and $d_Z = 0.05$.

Table S1. Results of multimodel inference conducted in the MuMIn package of R statistical software and treating metacercariae per *Rana pipiens* metamorph as the response variable

Effect	Estimate	SE	Adjusted SE	z value	Pr(> z)	Relative importance
Intercept	0.821	1.186	1.250	0.657	0.511	
Taxonomic richness of potential cercarial and snail predators	-0.344	0.121	0.131	2.619	0.009	0.96
Atrazine concentration	3.146	1.218	1.319	2.385	0.017	0.94
Phosphate concentration	0.380	0.236	0.253	1.502	0.133	0.19
Pigmented melanomacrophage score	-1.278	0.936	1.025	1.248	0.212	0.11
Wetland area	0.257	0.213	0.233	1.102	0.270	0.09
Species richness of snails	0.116	0.110	0.120	0.963	0.336	0.07
No. of <i>Planorbella trivolvis</i>	-0.001	0.013	0.014	0.054	0.957	0.07
Species richness of amphibians	0.062	0.103	0.112	0.550	0.582	0.05
Nitrate concentration	-0.088	0.190	0.208	0.422	0.673	0.04
Species richness of vegetation	0.011	0.028	0.030	0.358	0.720	0.04
Calcium concentration	<0.001	<0.001	<0.001	0.239	0.811	0.04

Table S2. Jackknife results for the relationship between larval trematode abundance per frog per wetland ($n = 18$ wetlands) and the richness of potential cercarial predators when all taxa of potential cercarial predators were included and when taxa were serially removed from the dataset to evaluate the sensitivity of the results to the presence of particular taxa

Dataset	r	P
All taxa included	-0.667	0.002
All taxa but		
Amphipods	-0.631	0.005
Dytiscidae	-0.614	0.007
Hydrophilidae	-0.605	0.008
Chaoboridae	-0.619	0.006
Belostomatidae	-0.664	0.003
Corixidae	-0.566	0.014
Nepidae	-0.646	0.004
Notonectidae	-0.693	0.001
Pleidae	-0.654	0.003
Aeshnidae	-0.736	0.001
Coenagrionidae	-0.545	0.019
Unidentified dragonfly	-0.607	0.008
Libellulidae	-0.691	0.001
Damselflies	-0.707	0.001
Dragonflies and damselflies	-0.678	0.002

Table S3. Results of general linear models examining the effects of odonate density (6 or 12 odonates) and odonate diversity (one to three species) on the abundance of three species of metacercariae and total metacercariae per *Rana clamitans* tadpole

Effect	(F/R)	df	Log Plagiorchidae				Log <i>Echinostoma trivolvis</i>				Log <i>Ribierioia ondatrae</i>				Log total metacercariae			
			β	SE	F	P	β	SE	F	P	β	SE	F	P	β	SE	F	P
Block	Random	1,45	0.414	0.126	10.79	0.002	0.171	0.137	1.55	0.219	-0.708	0.099	51.14	0.000	0.321	0.130	6.47	0.014
Log density	Fixed	1,45	-1.195	0.499	5.73	0.021	-1.230	0.545	5.10	0.029	-0.270	0.393	0.47	0.495	-1.309	0.517	5.82	0.020
Log diversity	Fixed	1,45	-1.883	0.926	4.14	0.048	-2.187	1.010	4.68	0.036	-0.307	0.728	0.18	0.676	-2.129	0.959	4.16	0.047
Log density * log diversity	Fixed	1,45	2.096	1.044	4.03	0.051	2.646	1.140	5.39	0.025	0.188	0.821	0.05	0.820	2.354	1.082	4.08	0.050